Materials & Design 218 (2022) 110681

Contents lists available at ScienceDirect

Materials & Design

journal homepage: www.elsevier.com/locate/matdes

D-optimal design of experiments applied to 3D high-performance concrete printing mix design

Vasileios Sergis, Claudiane M. Ouellet-Plamondon *

École de technologie supérieure, Université du Québec, Construction Engineering Department, Montréal, QC H3C 1K3, Canada

HIGHLIGHTS

- The methodology helped to greatly reduce the number of mixes, from $729\left(=3^6\right)$ to 18.
- The most important factors were identified as well as the levels in a mix design with high complexity.
- Achievement of high compressive strength, shape stability and flowability simultaneously.

GRAPHICAL ABSTRACT

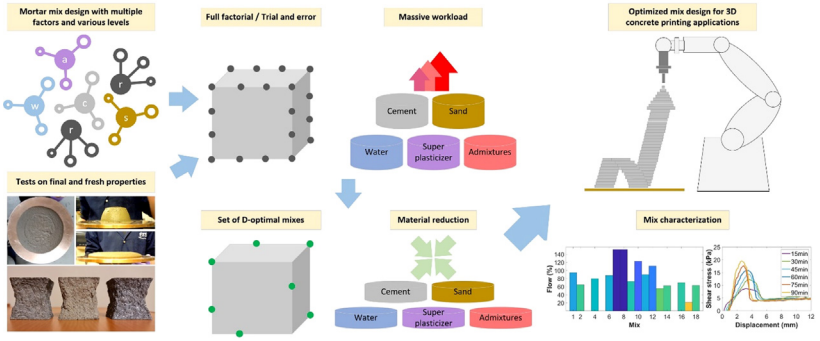

ARTICLE INFO

Article history:
Received 5 November 2021
Revised 15 April 2022
Accepted 18 April 2022
Available online 22 April 2022

Keywords:
Mix design
Optimal mix design
Design of experiments
D-optimal design
Multiobjective optimization
3D concrete printing

ABSTRACT

The development of 3D printable cement-based materials is a complex process with a variety of competing objectives. The compositions formed are far more complex than in conventional concrete, increasing the difficulty in designing mixtures for 3D concrete printing. As the number of materials in mix design increases, the workload increases exponentially during the development process. In this study, the D-optimal experimental design method is employed to reduce the number of experiments while providing statistically grounded designs with high-quality results. The proposed D-optimal design includes 18 mixes that investigate three level-six factors. High-performance cementitious printing mortar was selected for future applications of new thinner structures with less massive concrete. In total, three types of cement, three types of sand and five admixtures are investigated, including superplasticizers. The factors are the cement, sand, and superplasticizer type, the water-binder and sand-binder ratio, and the use of a viscosity modifying agent or C-S-H seed admixture. Calorimetry tests were conducted along with the direct shear test, the flow test and the compressive strength test. Results indicated that a D-optimal mix design can reduce the required workload while assessing the importance of each factor and level included in a mix design with high complexity.

1. Introduction

3D printing technology is gaining interest in the construction industry. The flexibility to construct freeform shapes without using formwork is one of the biggest advantages of this technology [1,2]. Researchers are seeking the best materials in the mix design to coordinate the cement hydration mechanisms and the operations

* Corresponding author.
E-mail address: Claudiane.Ouellet-Plamondon@etsmtl.ca (C.M. Ouellet-Plamondon).

https://doi.org/10.1016/j.matdes.2022.110681
0264-1275/

of pumping, material deposition and curing. In most studies, the mass proportion of aggregate is in the range of 45–55%, which is very low when compared to conventional concrete, typically containing more than 75% of aggregate [3–8]. The average water-to-binder ratio can also be estimated to be around 0.3 %w. Frequently, a portion of the cement is replaced by fly ash and silica fume. Fly ash improves pumpability and extrudability while silica fume improves thixotropy and buildability. Various types and dosages of chemical admixtures and rheological modifiers are used depending on the application and the required performance of the mixture. Superplasticizers, accelerators, retarders, viscosity modifying agents, nano-silica, and fibers are a few examples [3]. The development of 3D printable cement-based materials is a complex process with a variety of competing objectives [9]. For printed materials with extrusion systems, high flowability before deposition, high extrudability and buildability at the time of the deposition, and high stiffness immediately after the deposition are desirable [10,11]. The necessity to acquire all those properties results in compositions that are far more complex than in conventional concrete, increasing the difficulty in designing mixtures for 3D concrete printing. Additional complexity is added due to the vital need for recycling and reusing products used in construction [1,12–14]. For instance, the use of recycled glass cullets reduces sand demand while also providing a solution for waste glass. According to studies, using recycled glass cullets improves flowability, but compromises are made in terms of buildability and mechanical properties [15,16].

Various methodologies are used in a mix design, such as changing one factor at a time or following a full-factorial plan [17,18]. In fact, the mix design methods differ, as do the ingredients used. Currently, the number of studies investigating mix design methods is quite limited. The mixture proportion is frequently given directly, with no design method or explanation of how the parameters were obtained. The two main methodologies proposed are the empirical mix design and the mix design following a rheological model [3]. The trial-and-error method of mix design is straightforward and effective [19–21]. However, with the increase of the factors or the levels of the factors in a mix design, the number of experiments increases exponentially [22,23]. As a result, the main compositions of the mix, such as cement, sand, or water, remain constant in most studies. Only a few parameters, such as admixture dosage, are treated as independent variables in order to find the best mix. Although studies with up to five independent variables or factors used regression models as guidelines, a massive workload was still required [24,25]. Other researchers have created rheological models to predict the static yield stress of the mixes based on the components selected [26,27]. In this approach, the mortar is regarded as a diphase composite material consisting of cement paste and sand. When compared to trial-and-error methods, yield-stress-based mix design methods have significant advantages. However, because these models were developed under specific experimental conditions, they cannot be directly applied to mix design for 3D concrete printing applications [3].

The flowability of the mix is one of the most important properties [17,21,28]. Slump and flow tests are used to define the printable region and the buildability of the mixes [17]. The buildability of the mixes can be evaluated in terms of the maximum height printed before collapsing. The water-to-binder ratio and sand-to-binder ratio affect the flowability and buildability. Mixtures with a slump flow value between 50% and 90% give a smooth surface and high buildability [17]. The material yield stress should be within a range of 1.5–2.5 kPa to achieve extrudability and buildability [21]. Otherwise, the material may not achieve shape stability, or the extrudability will be reduced. The open time of the mixture increases with silica fume or a viscosity modifying agent, and the yield stress can be increased with a viscosity modifying agent or silica fume [21]. The time window of the mixes has the same importance, and the hydration process can provide insight into the setting time [29,30]. Through the isothermal calorimeter, the setting time of cement-based materials can be predicted from the first derivative of the heat evolution curve [29], and good correlations are observed with those from the ASTM C403 tests. The setting times are proportional to the water-to-binder ratio and inversely proportional to the cement fineness, but the results may vary among different cements [30]. Researchers tend to give more emphasis in fresh properties with less consideration of the mechanical properties, although this is not always true. The compressive strength is one of the most important mechanical properties [31,32]. Mixes with significant mechanical strengths are a target for 3D printing [33,34]. The highest compressive strength is measured in the perpendicular load direction. The compressive strength of high-performance 3D printed specimens can be 75 to 102 MPa when the compressive strength in casted molds for the same mix is 107 MPa [34]. While the final properties are always crucial, for this technology, the early age structural buildup and strength development during the dormant period is equally important [35–38]. Geotechnical tests, such as the direct shear test, have been used to acquire the properties in fresh-state mortar mixes. A timespan of 0–90 min is recommended for testing, with time intervals of 15–30 min [36]. A shear stress of 8.9 kPa was achieved after 90 min in the mixture used in this study, where the structure started collapsing after 40 successive layers. Another study claims that the shear rates do not have a large impact in the direct shear test and that the cohesion of the mixes is proportional to the binder-to-sand ratio [37].

The study attempts to address the question of whether the design of experiments (DoE) can add value to the mix design in 3D concrete printing. DoE is a mathematical tool to plan and analyze experiments. The combination of this tool along with optimization algorithms and artificial intelligence has the potential to reduce the material and time required to develop a mix with the desirable properties. The D-optimal design was selected to create the initial set of mixes [39]. This is a nontraditional experimental design that can drastically reduce the number of experiments and provide statistically grounded designs with high-quality results. More details is found in Atkinson and Donev [40]**.** Following a multiobjective approach, the overall objective is to develop a flowable material that will allow good printing speed and thin structures for 3D concrete printing applications. Flowability depends on the extrusion system used. Mixes with high flowability will be pumped more easily, but this will be at the expense of buildability. Structural buildup in the dormant period is critical for 3D concrete printing. Aiming for high printing speeds, the shear stress should be as high as possible, although compromises need to be made in terms of flowability or the mechanical strength. As with the buildability and shear stress, the goal is also to increase the hardened properties to the maximum extent possible. Achieving high-performance cementitious printing mortar enables future applications to use thinner structures with less massive concrete. In total, three types of cement, three types of sand and five admixtures are investigated in this study, including superplasticizers. The factors are the cement, sand, and superplasticizer type, the water-binder and sand-binder ratio, and the use of a viscosity modifying agent or C-S-H seed admixture. Previous results [18] were analyzed to determine which admixtures would be used in the new mix design [41]. The calcium silicate hydrate (C-S-H) admixture is a strength-enhancing admixture that improves both the early and late-age strength development in concrete. The biopolymer polysaccharide viscosity modifying agent can control the rheological properties of the mixtures. Three types of superplasticizer are selected, two based on synthetic organic polymers such as polycarboxylate ether, and the other one based on sulfonated naphthalene

polymer. Four properties are investigated for the selected materials, namely, the flowability, buildability, open time and mechanical strength. The proposed testing methods are the ASTM C1679 calorimetry test, the ASTM C1437 flow test, the ASTM D3080 direct shear test and the ASTM C109 compressive strength. Section 2 of the paper presents the mix design, the selected materials and the testing methods in more detail. Section 3 outlines the results obtained in terms of the material properties. Section 4 concludes the study and summarizes the results. The D-optimal mix design and the proposed methodology showed promising results in reducing the material and time required to assess the importance of each factor and level included in a mix design with high complexity.

2. Materials and testing methods

2.1. Testing methods and equipment used

The proposed testing methods are the calorimetry test, the flow test, the direct shear test and the compressive strength. Those four were deemed adequate to start with and to see which can help draw important conclusions regarding the workability and flowability of the material, the early resistance of the mix during the first few minutes, its setting time and its compressive strength.

The ASTM C1679 calorimetry tests [42] can provide insight into the hydration process and compare the different mixes in terms of the produced heat, delay in the hydration peak or estimated setting time. A calorimetry test was performed to observe the hydration process and estimate the final setting time of the mixes [29,30]. The channels are of the twin type, consisting of a sample and a reference chamber. Each channel accommodates ampoules with a 20 mL volume. The operating temperature was 25 °C, and the test was conducted for 48 h. Mixing took place outside of the calorimeter using an advanced and high-speed overhead stirrer. The stirring speed was 2000 rpm, and the mixing time was one minute. Then, 4.0 mL of the mixture was placed inside the ampoule, sealed and placed inside the calorimeter to start the baseline. The measurement started 45 min after mixing on average.

From the ASTM D3080 direct shear test [43], strength development can be observed during the dormant period. The more resistance the material has, the better it is. Following a similar methodology where the same test was performed [35,36], multiple tests were conducted within 90 min, with a time interval of 15 min (15, 30, 45, 60, 75, 90 min after mixing). The direct shear apparatus generally used in soil mechanics was modified instead of creating a new apparatus as in the reference study. The modified apparatus consisted of a shear box, a displacement sensor, a load sensor and a linear displacement motor. The displacement rate was 12.7 mm/min, which simulates the vertical printing speed. The shear box consisted of a cup, the upper and bottom parts, and two bolts to keep the two parts connected (Fig. 1). Each specimen was placed in two layers of equal size (approximately 80 g for each layer), and a vibrating plate was used to consolidate the layers and remove the air voids. The collected data were the load and displacement of the specimens with a 1.5 N normal load, including the cup weight and the half-weight of the specimen. For each mix, all the specimens were prepared at the same time, and the process took 8 min after the mixing procedure. Each test lasted less than 2 min.

The ASTM C109 compressive strength [44] provides information about the final properties. Two inches or 50 mm test cubes were prepared and compacted by tamping in two layers. Three cubes were prepared for each test for repeatability. Bronze cube molds were used with wing nuts and studs, which secured the mold halves together and clamped the base to the mold body. The cubes were cured for one day in the molds, stripped and placed in a room where the temperature and humidity were controlled for seven and 28 days. The relative humidity was 97.5%, and the temperature was 22 °C on average. A semiautomatic concrete compression machine with a hydraulic piston was used to perform the test. In the beginning, the piston rises at a high speed until the specimen touches the upper platen. The piston then maintains the preset pace rate, which was 1 kN/s. When the specimen reaches failure, with subsequent release of the oil pressure, the maximum load is reached. The pictures of the undamaged test specimen central core show satisfactory compressive strength results (Fig. 2) [45].

The last test is related to the workability and flowability of the mixes. The ASTM C1437 flow test [46] allow to measure the spread of the mixes and to correlate the results with the pumpability of the mixes. The pumpability can be seen as the mix volume that can be pumped within 30 s [17]. For each specimen, a truncated cone was placed at the center of the flow table. The specimen was prepared and compacted by tamping in two layers. The truncated cone was then removed, leaving the mortar sample, which was dropped 25 times within 15 s, maintaining a steady pace. The diameter of the specimen was measured along the four lines scribed on the flow table using a caliper that conforms to the specification of the ASTM C230/C230M norm. The flow of each specimen was equal to the addition of the four readings, within 0–152%. The flow is the resulting increase in average base diameter of the mortar mass, expressed as a percentage of the original base diameter. Multiple tests were conducted within 90 min, with a time interval of 15 min (5, 15, 30, 45, 60, 75, 90 min after mixing). Two cameras were placed, capturing a side and the top view, to inspect the behavior of each mixture over time (Fig. 3).

2.2. Mix design and materials used

The selected admixtures were the two most significant admixtures from a previous study [41] and three superplasticizers or admixtures with water-reducing effects. The calcium silicate hydrate admixture is a strength-enhancing admixture that improves both the early and late-age strength development in concrete. This admixture improves the hydration of Portland cement with a stable suspension of synthetically produced crystalline calcium silicate hydrate (CSH-C) nanoparticles. Depending on the desired properties of the mix, it either reduces the number of cementitious materials or creates structures with high strength

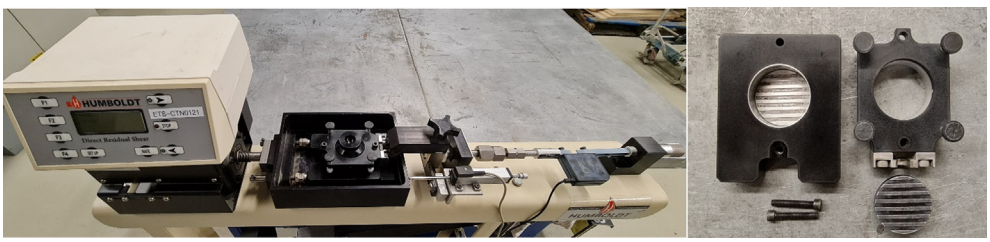

Fig. 1. Direct shear test apparatus used in soil mechanics modified with a 100 N load sensor and 20 mm displacement sensor.

Fig. 2. Cubes specimens after measuring compressive strength. GU with coarse sand, HE with fine sand, GUbSF with recycled sand.

[33,34]. The biopolymer polysaccharide viscosity modifying agent (B) can control the rheological properties of the mixtures. A few examples are that it provides stability, thixotropic properties and consolidation, enhances the viscosity and makes the mix less prone to segregation. Among the three selected superplasticizers, two are based on synthetic organic polymers such as polycarboxylate ether (PCE). The third superplasticizer is a water-reducing and accelerating admixture that is sulfonated naphthalene polymer based. The latter can reduce permeability, shrinkage and creep and increase the workability and modulus of elasticity. For cement, the three types are general use Portland cement (GU), Portland cement with high early strength (HE) and binary cement with silica fumes (GUbSF). The chemical analysis of the cement types is presented in Table 1, as provided by the local supplier.

For the sand, all three types were fine aggregates with particle sizes below 2.5 mm. However, each one has different characteristics, as the first one is finer, the second coarser and the third one is recycled sand that was collected from the residues from the sedimentation basin of truck concrete mixer washing facilities. The particle size distribution is presented in Table 2. The recycled sand is closer to the coarse sand, but it is evenly distributed with more particles above 1.25 mm and below 315 μm than the coarse sand.

The mix design is highly dependent on the application. A different mix design will be required for an underground, indoor or outdoor application. For the latter, different mix designs are required for different climates. Regardless of the application, the factors of the mix design are related to the mixing process, the equipment used and the selected materials. The initial factors for this study were six with three levels each, all related to the selected materials. These factors are the cement type, sand type, water-to-binder ratio, sand-to-binder ratio, superplasticizer type and use of a second admixture [47]. Table 3 shows the proposed levels for each factor.

Here, GU refers to the general use Portland cement, HE to Portland cement with high early strength, and GUbSF to binary cement with silica fumes (ASTM C1157). The PCEs are superplasticizers based on synthetic organic polymers, and the SNP is a sulfonated naphthalene polymer-based water reducer. Finally, B refers to the addition of a biopolymer polysaccharide viscosity modifying agent, and CSH-C refers to the addition of crystalline calcium silicate hydrate. The dosage for all admixtures is the median value of the manufacturer's recommended dosage. The particle size of all the sand types is below 2.5 mm.

A full factorial plan for the selected number of factors and levels would require $3^6 = 729$ experiments to be made per test. The number of experiments would be impractical even if a fractional factorial plan were used. The benefit of using a D-optimal design is that the required runs and the amount of resources and time will be drastically reduced. The designer can choose the number of mixes that he or she wishes to form. This class of experimental designs selects the best group of design points with respect to a statistical criterion. This methodology can provide statistically grounded designs with high quality results which can be obtained with a reduced number of experimental runs compared to non-optimal designs. D-optimal design criteria seek to maximize |X'X|, the determinant of the information matrix X'X, or to minimize the generalized variance of the estimated regression coefficients [39]**.** The matrix X represents the data matrix of the independent variables, where the columns are the model terms and the rows the experiment runs. The D-optimal design is created through a computer with an iterative search algorithm. For this study, 18 mixes were selected with a D-efficiency equal to 100%. These 18 mixes were the initial set for a multiobjective optimization algorithm aiming to improve the properties. R software and the available libraries were used, such as the gen.factorial function in the package DoE. base and the optFedeov function in the package AlgDesign [23]. The gen.factorial function was utilized to create an orthogonal array set of candidates, and the optFedeov function was used to select an 18-run D-optimal subset. The output is an 18x6 table with integer values. The columns were the factors, the values the levels of each factor and the rows the optimum treatment runs or mixes. After the integer values were converted into the selected materials for this mix design, Table 4 was formed.

2.3. Multiobjective approach and goals

For 3D printing applications, the optimum material should have high flowability before deposition, high extrudability and buildability at the time of the deposition, and high stiffness immediately after the deposition [11]. Apart from the fresh properties that are crucial, the aim was also to achieve the highest possible compressive strength. Various other criteria could be given in a multiobjective approach, but for simplicity and proof of concept of this methodology, only those criteria were respected. Specifically, the goals that were set are the following.

- Flowability: Flowability depends on the extrusion system used. Increased flowability will be pumped more easily, but it comes in contrast to buildability. The threshold set for this study is a mortar flow above 60%, 5 min after the end of the mixing process.
- Shape stability/Buildability: Structural buildup in the dormant period is crucial. Aiming for high printing speeds, the shear stress should be as high as possible, but compromises will be made for the other two objectives. In this study, a threshold of 16 kPa in 90 min after mixing was set.

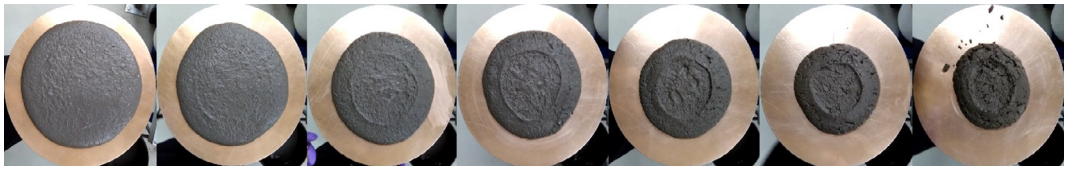

Fig. 3. ASTM C1437 flow test performed within 90 min, with a time interval of 15 min.

Table 1
Chemical analysis (%) of the general use Portland cement (GU), Portland cement with high early strength (HE) and binary cement with silica fumes (GUbSF).

Cement	SiO_2	Al_2O_3	Fe_2O_3	CaO	MgO	SO_3	Loss on ignition	Total alkali
GU	19.1	4.8	3.6	60.2	2.6	3.8	1.9	0.92
HE	19	4.8	3.6	60.4	2.6	4.4	1.8	0.94
GUbSF	27	4.2	1.6	57.5	1.6	3.6	3	0.73

Table 2
Particle size distribution of the fine, coarse and recycled sand.

	Passing through (%)		
Sieve size	Fine sand	Coarse sand	Recycled sand
2.5 mm	100	100	100
1.25 mm	90	96	83
630 μm	78	67	66
315 μm	57	24	34
160 μm	20	4	12
80 μm	3	3	5

- Mechanical properties: A threshold of 80 MPa after 28 days was set for the compressive strength of high-performance concrete. As with the buildability and shear stress, the aim was to increase the hardened properties as much as possible.

Only the mixes that respect these criteria were considered accepted.

3. Results and discussion

3.1. Cement hydration

A good comprehension of the chemical and physical processes of cement hydration is vital to acquire a better understanding of the influence of concrete admixtures on the properties of fresh and hardened concrete. In this study, an isothermal calorimetry was used. For those tests, four factors were considered instead of six because the tests were made on cement paste specimens. These parameters were the cement type, the water-to-binder ratio, the superplasticizer type and the use of a second admixture. The collected data can be seen in Fig. 4, where the tests are grouped by cement type. Each graph includes the results of six mixes, except for Fig. 4c, in which the heat flow curves of five mixes are presented. The reason was that the test for mix 15 could not be performed due to the fast setting and low flowability of the mixture. The addition of CSH-C increases the heat flow during the acceleration period (mixes 3, 12, 8, 16 and 4, 14) and increases the setting time. On the other hand, the addition of B has a negligible effect on the setting time or the heat flow. The third type of superplasticizer SNP reduces the setting time, even in mixes that include CSH-C (mixes 2, 3, 9, 18 and 14). Additionally, the PCE-1 superplasticizer has a quicker setting time than PCE-2. To estimate the initial setting time of the mixes, the first derivative of the heat flow with respect to time is calculated. The highest point is approximately the initial setting time [29,30]. The results are presented in Table 5, where the observations regarding the setting time can be verified. For instance, the average setting time for the mixes where the SNP superplasticizer was used is 5 h and 52 min, whereas the average setting time of the mixes with PCE-1 and PCE-2 are 10 h 15 min and 11 h 07 min, respectively.

3.2. Direct shear test

The time required for a test to be executed on fresh mortar specimens is crucial to eliminate the influence of thixotropic buildup during the test. The direct shear test meets this criterion, and the ease of repeatability of the test allows us to acquire shear stresses of the same mixture with 15-minute time intervals. The collected data were the load and displacement of the specimens with a 1.5 N normal load, including the cup weight and the half-weight of the specimen. The behavior varied over time and for the different mixes. In the beginning, the load is increased proportionally to the horizontal displacement, showing plastic behavior until reaching the highest peak. After the peak, as the deformation grows, the load is gradually reduced. A more brittle failure is observed as the age of the specimen increases. Among the 18 mixes, mix 4 (HE|Fine|0.345|2.0|PCE-2|CSH-C) was one of the best-performing mixes. In Fig. 5a, the force–displacement graph of the 4th mixture is presented. After the peak, in the first tests, the force gradually decreased, while in the last tests, there was a sudden drop in the resistance of the specimen. The collected data were converted into a shear stress displacement graph. The results for the 4th mixture are shown in Fig. 5b.

A shear stress displacement graph was created after the correction of the cross-sectional area of the specimen during the test [48]. As the direct shear test progresses, the area that comes in contact with the upper and lower parts of the specimen diminishes. The area can be calculated from Eq. (2) [48]:

$$A = A_0 \frac{2}{\pi}\left\{\cos^{-1}\left(\frac{\Delta h}{D}\right) - \left(\frac{\Delta h}{D}\right)\sqrt{1-\left(\frac{\Delta h}{D}\right)^2}\right\} \quad (2)$$

where

- A_0 is the full cross-section of the specimen;
- D is the diameter of the specimen;
- Δh is the horizontal displacement.

The shear stress displacement for all the mixes is shown in Fig. 6, grouped by the time when the tests were conducted. The shear stress is defined for each test as the maximum occurring stress after area correction, Eq. (2), and is summarized in Table 5. The acceptable shear stresses above 16 kPa at t = 90 min was given from mixes 2, 4, 13, 14 and 18. The presence of the SNP superplasticizer can be observed in most of those mixes. Additionally, the combination of the HE cement, the PCE-2 superplasticizer and a type S admixture gave acceptable results.

Table 3
Materials selected for the mix design.

Cement	Sand	Water-binder ratio	Sand-binder ratio	Superplasticizer (Type A&F)	Type S admixtures
GU	Fine sand	0.32	1.8	PCE-1	–
HE	Coarse sand	0.345	2	PCE-2	B
GUbSF	Recycled sand	0.37	2.3	SNP	CSH-C

Table 4
The 18 mixes from the D-optimal mix design.

Mix	Cement	Sand	Water:binder	Sand:binder	Superplasticizer (Type A&F)	Type S admixtures
1	GU	Coarse	0.320	1.8	PCE-1	–
2	GU	Coarse	0.345	2.0	SNP	B
3	GU	Fine	0.320	2.3	SNP	CSH-C
4	HE	Fine	0.345	2.0	PCE-2	CSH-C
5	HE	Fine	0.370	2.3	PCE-1	–
6	HE	Recycled	0.345	1.8	PCE-1	B
7	GUbSF	Coarse	0.370	2.0	PCE-2	–
8	GUbSF	Recycled	0.320	1.8	PCE-2	CSH-C
9	GUbSF	Recycled	0.370	2.3	SNP	B
10	GU	Fine	0.370	1.8	PCE-2	B
11	GU	Recycled	0.345	2.3	PCE-2	–
12	GU	Recycled	0.370	2.0	PCE-1	CSH-C
13	HE	Coarse	0.320	2.3	PCE-2	B
14	HE	Coarse	0.370	1.8	SNP	CSH-C
15	HE	Recycled	0.320	2.0	SNP	–
16	GUbSF	Coarse	0.345	2.3	PCE-1	CSH-C
17	GUbSF	Fine	0.320	2.0	PCE-1	B
18	GUbSF	Fine	0.345	1.8	SNP	–

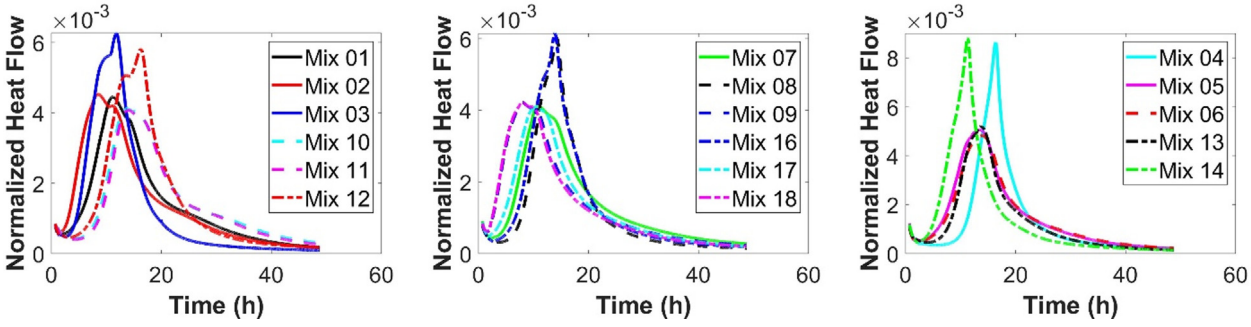

Fig. 4. The normalized heat of the mixes with GU (a), GUbSF (b), and HE (c) within the first 48 h.

Table 5
The properties of the 18 mixes.

Mix	Mix description	Flow in 5 min (%)	Initial setting time (h min)	Shear stress in 90 min (kPa)	Compressive strength in 28 days (MPa)
1	GU|Coarse|0.32|1.8|PCE-1|-	95	9 h 33	12.0	81.3
2	GU|Coarse|0.345|2.0|SNP|B	65	4 h 25	20.6	66.7
3	GU|Fine|0.32|2.3|SNP|CSH-C	0	6 h 24	–	–
4	HE|Fine|0.345|2.0|PCE-2|CSH-C	80	15 h 58	19.6	83.0
5	HE|Fine|0.37|2.3|PCE-1|-	0	9 h 49	–	–
6	HE|Recycled|0.345|1.8|PCE-1|B	88	10 h 17	12.5	81.1
7	GUbSF|Coarse|0.37|2.0|PCE-2|-	152	7 h 39	6.6	92.3
8	GUbSF|Recycled|0.32|1.8|PCE-2|CSH-C	152	10 h 08	7.6	102.2
9	GUbSF|Recycled|0.37|2.3|SNP|B	73	3 h 53	14.9	70.6
10	GU|Fine|0.37|1.8|PCE-2|B	123	11 h 26	9.3	76.9
11	GU|Recycled|0.345|2.3|PCE-2|-	90	11 h 21	9.3	78.9
12	GU|Recycled|0.37|2.0|PCE-1|CSH-C	111	11 h 30	11.2	78.1
13	HE|Coarse|0.32|2.3|PCE-2|B	56	10 h 07	21.1	80.7
14	HE|Coarse|0.37|1.8|SNP|CSH-C	63	10 h 52	19.1	66.6
15	HE|Recycled|0.32|2.0|SNP|-	0	–	–	–
16	GUbSF|Coarse|0.345|2.3|PCE-1|CSH-C	70	13 h 24	15.0	90.7
17	GUbSF|Fine|0.32|2.0|PCE-1|B	21	6 h 55	–	–
18	GUbSF|Fine|0.345|1.8|SNP|-	63	3 h 46	16.8	69.8

The effect of the materials on shear stress development during the first 15 min is difficult to observe. However, after 30 min, the shear stress median value of the HE cement type mixes is double that of the GU cement type mixes, with 13.9 and 6.74 kPa, respectively. The difference between the two cement types becomes apparent as the specimen age increases. At 60 and 90 min after mixing, the median values for the HE cement type are 15.84 kPa and 19.55 kPa, respectively, whereas the median values for the GU type mixes are 7.5 kPa and 11.97 kPa for the same specimen age. The GUbSF type mixes performed better than the GU type but worse than the HE type. The shear stress was gradually increasing, with no abrupt changes. As a comparison, the median value for the GUbSF type mixes at 90 min is 14.86 kPa, whereas the HE type mixes had a median value of 15.84 at 60 min after mixing. The type of superplasticizer was the second most important factor in the development of shear stress. For the first 60 min, the three types had nearly identical shear stress effects, with the PCE-2 type slightly ahead of the other two, with 13.26 kPa,

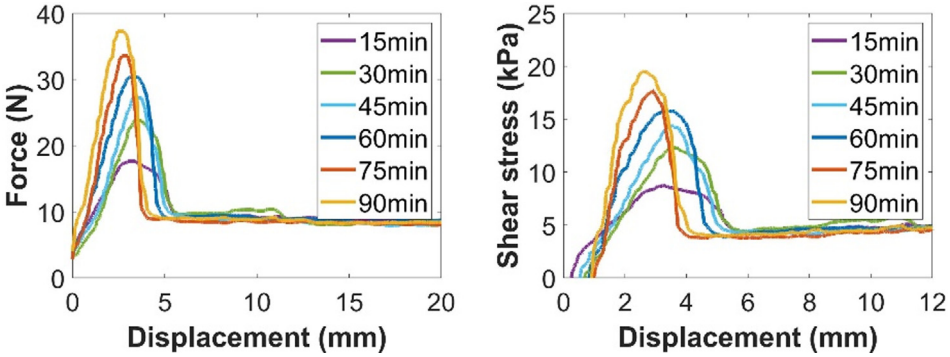

Fig. 5. The load displacement (a) and shear stress displacement (b) graphs of mix 4 within 90 min with 15 min time intervals.

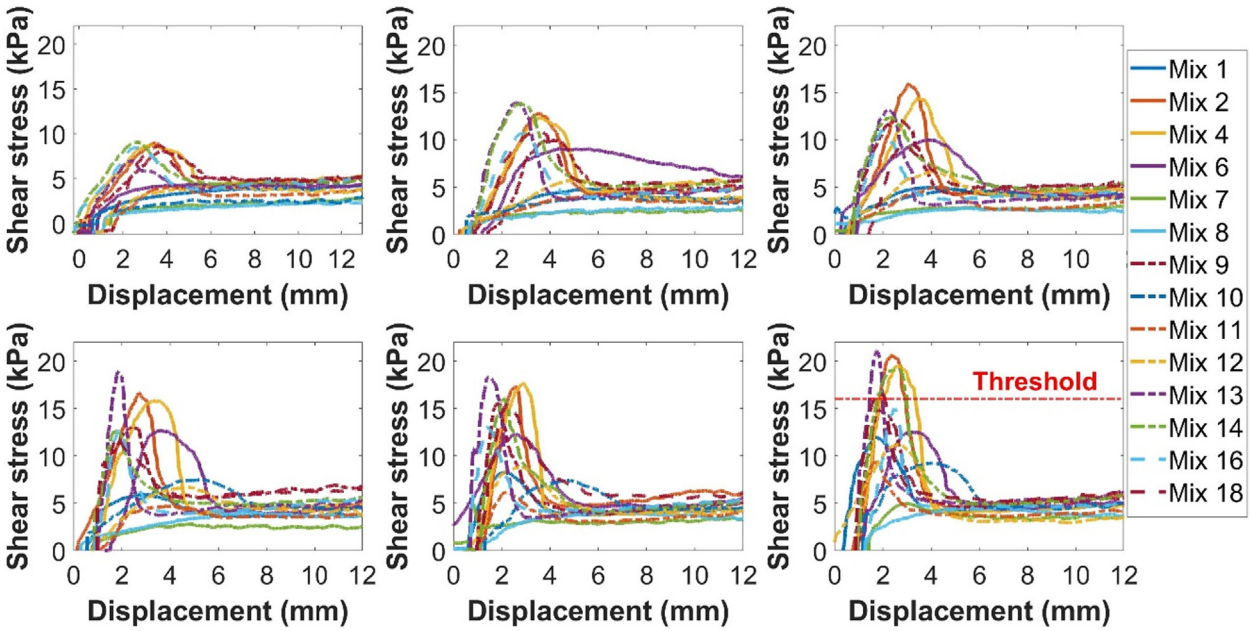

Fig. 6. Shear stress displacement graph of the mixes grouped by specimen age. The ages vary from 15 to 90 min, with 15-minute time intervals, beginning with the top row and left graph and progressing to the bottom right graph. The final graph depicts the buildability criteria, which is set at 16 kPa and is denoted by the threshold and the horizontal red dashed line. (For interpretation of the references to color in this figure legend, the reader is referred to the web version of this article.)

whereas the SNP had 12.81 kPa and the PCE-1 12.52 kPa. However, at 75 min, the SNP type increased rapidly, followed by the PCE-2, while the PCE-1 increased gradually. The mix-containing SNP, PCE-2, and PCE-1 had median values of 15.84, 14.38, and 12.63 kPa at 75 min and 17.97, 16.53, and 14.52 kPa at 90 min, respectively.

3.3. Flow test and compressive strength

There was a large variation in the spread depending on the mixes. The use of fine sand, HE cement, SNP superplasticizer, the lowest value of the water-to-binder ratio or the highest value of the sand-to-binder ratio resulted in mixes with a lower flow. Combinations of those options resulted in dry mixes that were unable to form a flowable mortar, such as mixes 3, 5 and 15. This created a problem to measure the rest of the properties, since it was impossible to form any specimens. On the other hand, mixes 7 and 8 were so liquid that the specimen was spread all over the flow table. The rest were in the range of a 20–125% spread increase in the diameter of the truncated cone. Based on the criteria regarding flowability, all the mixes were considered acceptable except for mixes 3, 5, 13, 15 and 17. In Fig. 7a, a color-coded bar graph summarizes the results of the flow tests 5 min after mixing. The results towards the dark blue color indicate the increase in flowability, whereas the green color indicate that the mixes are close or below the acceptable threshold of 60% spread increase in the diameter of the truncated cone.

Even if the flow of the mixes was not the same and not always between 110% ± 5%, as specified in the ASTM norm, the same amount of energy was used to prepare the specimens by using a vibrating plate to consolidate the layers and remove the air voids. In Fig. 7b, the results towards the dark blue color indicate the increase in the compressive strength. The average compressive strength after 28 days of the formed mixes was close to 80 MPa, which was also the criterion for acceptable mixes (Fig. 7b). This test helped to indicate the mixes that performed better than the others and to discriminate the factors and the levels that improved the compressive strength. Acceptable results, which were above 80 MPa after 28 days, were obtained for mixes 1, 4, 6, 7, 8, 13 and 16. A closer look at those mixes reveals that the majority of them include the HE or GUbSF cement, the coarse sand or the recycled sand, the lowest values in both the water-to-binder and sand-to-binder ratio, the new generation PCE superplasticizers, and the addition of CSH-C. The results are presented in Table 5.

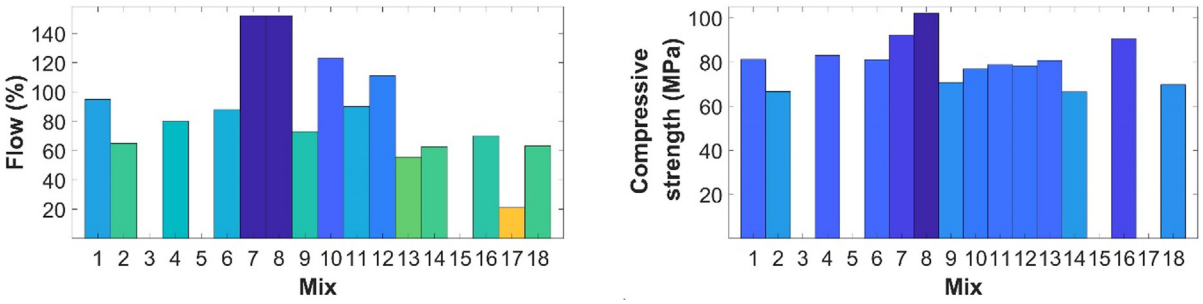

Fig. 7. Bar graph of the flow tests 5 min after mixing for all mixes (a) and the compressive strength after 28 days (b).

3.4. Analysis and discussion

The use of the D-optimal design methodology helped to greatly reduce the number of mixes, from $729\left(=3^6\right)$ to 18. However, three of the selected mixes were unable to be formed. Those mixes were too dry, making it impossible to measure all their properties. This was something to be expected in the initial set of mixes. The flow was the only property that was measured for all the mixes, regardless of whether they were able to be formed, with a range of 0–152%. The initial setting time could be measured for all of the mixes except for mix 15, where a fast setting was observed. For the shear stress and the compressive strength, the 3rd, 5th, 15th and 17th mixes were unable to be measured due to the low flow. The results are summarized in Table 5. Figs. 8–13 are the mean plots based on the collected data from the D-optimal design. These plots show whether the mean varies between different levels of each factor variable. The figures are grouped by factor, meaning the cement type, the water-binder ratio, superplasticizer type, sand type, sand-to-binder ratio and the addition of a type S admixture. The three most important factors were the cement type, the water-to-binder ratio and the superplasticizer type.

Among the three levels of cement type used in this study, the high early strength cement (HE) was the one with the largest influence on most of the properties based on the results of the mean plots (Fig. 8). For instance, the use of HE evidently increases the shear stress after 90 min and decreases the flow after 5 min of the mixing process. The GU and the GUbSF have a lower initial setting time than the HE. They also tended to increase the flow and decrease the shear stress after 90 min. Regarding the compressive strength, the mixes with GUbSF gave higher values, as expected, followed by HE. Similar conclusions can be found in the literature except for the setting time, where the fineness of the cement accelerates the reaction and reduces the setting time [29,30]. As expected, the cement fineness decreases the flow due to the increased absorption, and the addition of silica fume increases the compressive strength as a result of the pozzolanic reaction [32,49–52].

The water-to-binder ratio as a factor can be considered normally as a continuous variable and not as a discrete variable. However, the selected discrete values (0.32, 0.345 and 0.37) were enough to observe the tendency. The flow is almost proportional to the increase in the ratio, whereas the compressive strength is inversely proportional (Fig. 9). The shear stress seems to have an optimal point in the middle value of 0.345 and then decreases. The effect on the initial setting time is negligible, since the mean plot (Fig. 9b) shows that the initial setting time remains almost the same in all values of the water-binder ratio. The water-to-binder ratio is one of the most important parameters in mix design, and various studies have been conducted with similar results. For instance, with an increase in the water-to-binder ratio, the workability increases, whereas the strength decreases [32,52–55].

The type of superplasticizer was the factor with the largest variation in the results among the levels (Fig. 10). The mixes with PCE-2 had the highest flow, whereas the mixes with SNP had the lowest flow. This was also observed in the initial setting time, where there was an accelerating effect in the mixes with SNP. The use of SNP significantly increased the shear stress but greatly reduced the compressive strength compared to the other two superplasticizers. The accelerating effect of the SNP superplasticizer used in this study resulted in a high shear stress. However, the efficiency of the new generation of superplasticizers is better than that of the old generation. Based on the literature, the compressive strength was reduced when the SNP superplasticizer was used, and the PCE superplasticizer was more efficient at increasing the workability [56–58].

Variability was also present among the sand types (Fig. 11). The recycled sand increases the compressive strength, although it reduces the shear stress. Mixes with coarse sand have better properties than those with fine sand. Fine sand tends to reduce the flow and compressive strength, whereas coarse sand seems to increase all the properties. The calorimetry tests were performed in cement paste, and as expected, the mean plot in Fig. 11b proves no effect of sand on the setting time. It may appear apparent because the type of sand was not tested with the calorimeter. The results are still presented to show the effectiveness of the mix design method based on DoE, which allows to draw valid conclusions. Different results would imply that the mean value of each level is biased

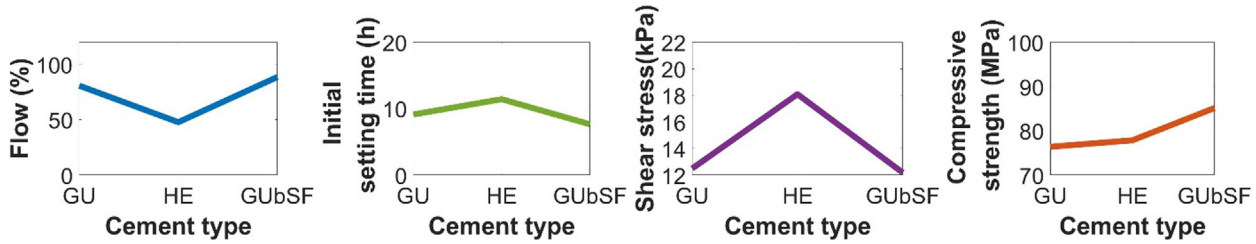

Fig. 8. The influence of the cement type on the measured properties flow (a), setting time (b), shear stress (c) and compressive strength (d).

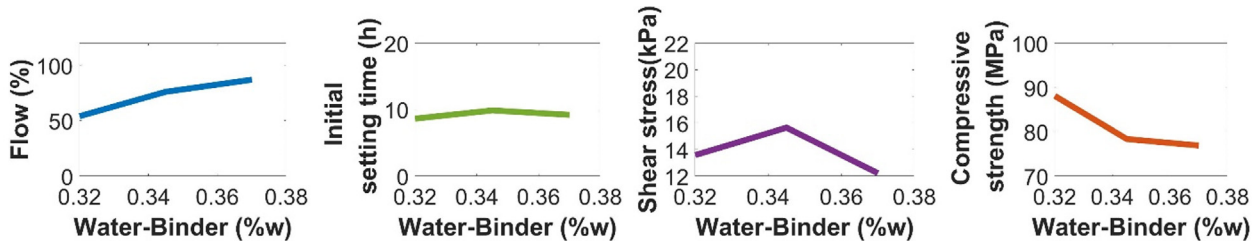

Fig. 9. The influence of the water-binder ratio on the measured properties flow (a), setting time (b), shear stress (c) and compressive strength (d).

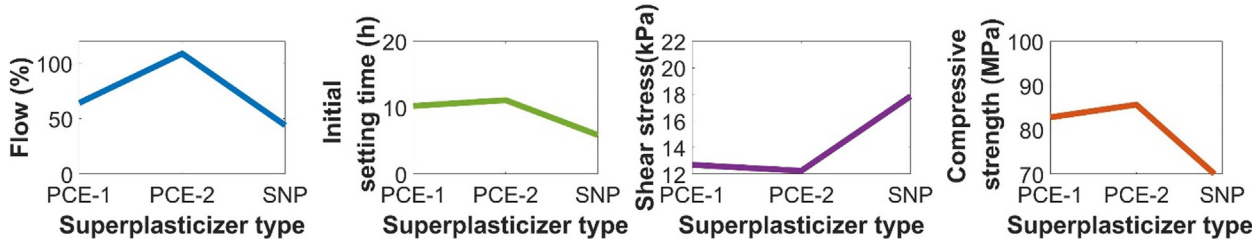

Fig. 10. The influence of the superplasticizer type on the measured properties flow (a), setting time (b), shear stress (c) and compressive strength (d).

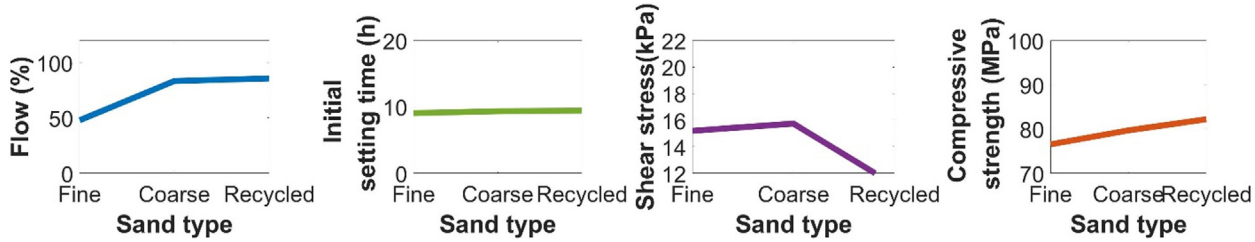

Fig. 11. The influence of the sand type on the measured properties flow (a), setting time (b), shear stress (c) and compressive strength (d).

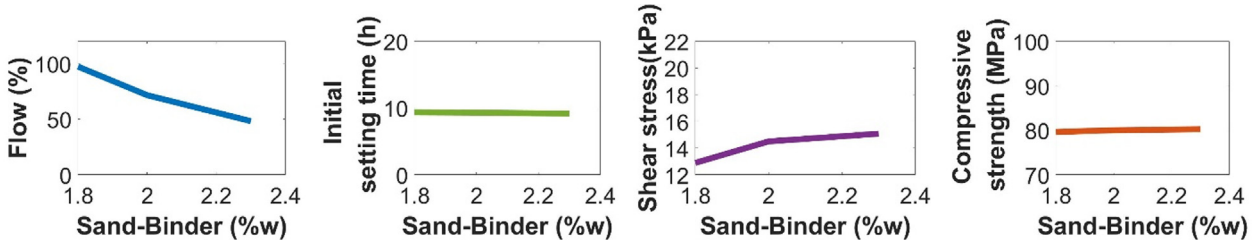

Fig. 12. The influence of the sand-binder ratio on the measured properties flow (a), setting time (b), shear stress (c) and compressive strength (d).

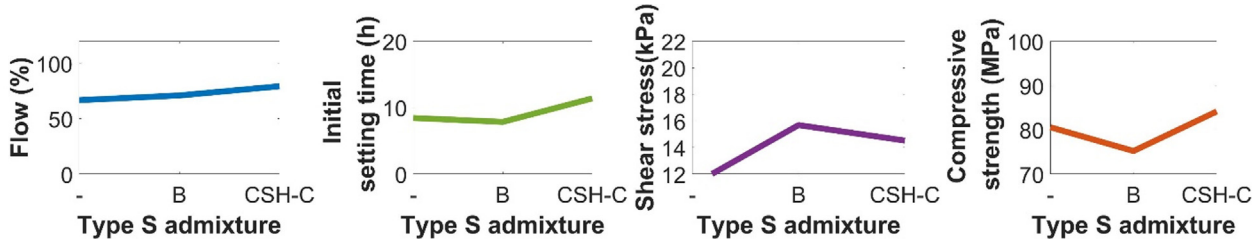

Fig. 13. The influence of the B and CSH-C admixtures on the measured properties flow (a), setting time (b), shear stress (c) and compressive strength (d).

by other factors or that the mix design does not treat all levels of the factors equally, which did not happen here. Studies suggest that the effective diameter of sand is proportional to the compressive strength and has a high effect on it [32,59]. The recycled sand had the second-highest effective diameter, approximately 0.16 mm, behind the coarse aggregate. The increased workability of the recycled sand can be explained by the rounded shape of the particles due to weathering. The shape of aggregates influences the workability, and by reducing the air voids, a higher workability should be expected [60].

As with the water-to-binder ratio, the sand-to-binder ratio is a factor that can be considered normally a quantitative factor instead of a qualitative factor, but for simplicity only three discrete values were observed at this phase of the study. The selected discrete values (1.8, 2 and 2.3) showed that the flow is inversely proportional to the increase in the ratio (Fig. 12). The shear stress seems to increase as the ratio increases. As with the sand type discussed previously, as expected, the mean plot in Fig. 12b proves that the sand-to-binder ratio has no effect on the setting time. The ratio also has a negligible effect on the compressive strength, as it remains stable within the three discrete values. According to the literature, the workability is expected to be reduced with the increase of the sand-to-binder ratio. The increase results in high porosity, which negatively influences the compressive strength [61]. Additionally, the cohesion of the mixes is proportional to the binder-to-sand ratio [21].

The sixth factor was the addition or absence of a second admixture. The options for a second admixture, other than the superplasticizer, were admixture B or CSH-C. The results for the mixes where admixture B was included showed that the shear stress was increased, whereas the compressive strength was reduced (Fig. 13). The flow was slightly increased, while the calorimetry test showed a decrease in the initial setting time. Studies suggest that the addition of viscosity-modifying agent admixtures increases workability. An increase in the yield stress and plastic viscosity should be expected. However, it does not help the compressive strength [50]. In contrast to the B admixture, the addition of crystalline calcium silicate hydrate (CSH-C) seemed to increase all the properties of the mixtures (Fig. 13). The increase in both the initial setting time and the compressive strength was evident. There was a slight increase in the flow and shear stress, although the increase in the shear stress was less than that of the B admixture. According to the literature, a substantial increase in compressive strength can be seen with the addition of CSH-C along with an acceleration of the hydration process [62].

A correlation between the flow of mortar specimens and the initial setting time of the cement paste specimens of the same mixes could not be made. Aiming to determine the flowability of the mixes, the flow test was deemed more suitable. Regarding the three objectives, to compare the mixes and define which one performed better, the values collected from the shear stress at 90 min and the compressive strength at 28 days were normalized. Aiming to increase both of these properties and respect the threshold of 60% flowability 5 min after the end of the mixing process, the two columns with normalized values were summed and normalized again from 0 to 1. The mixes were then sorted based on their performance, and those that did not meet the criteria of the flow, shear stress and compressive strength were rejected. Table 6 summarizes the results for the initial set based on the goals being set. From the 18 mixes, only the 4th mix met all the criteria, with 80% flow after 5 min, 19.55 kPa shear stress after 90 min and 82.99 MPa compressive strength after 28 days.

4. Conclusion

The contradicting objectives in the properties of the 3D cement-based mixes raise the challenge during the mix design process. This study shows that it is possible to reduce the workload required to assess the most important factors and levels included in a mix design containing six independent variables. The D-optimal mix design reduced the number of mixes required from a full factorial plan, from 729 to 18 mixes while allowing to draw important conclusions for each ingredient included in the mix design. The investigated factors were the cement, sand, and superplasticizer type, the water-binder and sand-binder ratio, and the use of a viscosity modifying agent or C-S-H seed admixture. Among the different materials that were used, it was possible to discriminate which of them had the largest influence on the flowability, shape stability and compressive strength of the mixture. Important conclusions were made, even with the high complexity of the mix design. The conclusions can be summarized as follows:

- The three most important factors were the cement type, the water-to-binder ratio and the superplasticizer type. The flow was almost proportional to the increase in the water-to-binder ratio, whereas the compressive strength was inversely proportional. The high early strength cement (HE) was the one with the largest influence compared to the GU and GUbSF. The type of superplasticizer was the factor with the largest variation in the results among the levels.
- The low water-to-binder ratio, the addition of CSH-C admixture, the recycled sand and the GUbSF cement increased the compressive strength. The effective diameter of sand has a high effect on the compressive strength, whereas the addition of silica fume increases the compressive strength as a result of the pozzolanic reaction.

Table 6
The 18 mixes sorted based on their performance.

Mixes sorted by best performance	Mix #	Flow (%)	Shear stress (kPa)	Compressive strength in 28 days	Normalized performance on shear and compressive strength	Flow $\geq$ 60%	Shear $\geq$ 16 kPa	Compressive strength $\geq$ 80 MPa	All objectives (AND)
1	M13	55.5	21.12	80.70	1.00	0	1	1	0
2	**M4**	**80**	**19.55**	**82.99**	**0.97**	**1**	**1**	**1**	**1**
3	M2	65	20.64	66.66	0.91	1	1	0	0
4	M16	70	15.01	90.72	0.89	1	0	1	0
5	M14	62.5	19.13	66.55	0.87	1	1	0	0
6	M18	63	16.79	69.78	0.83	1	1	0	0
7	M9	73	14.86	70.64	0.78	1	0	0	0
8	M6	88	12.52	81.05	0.77	1	0	1	0
9	M1	95	11.97	81.29	0.76	1	0	1	0
10	M8	152	7.63	102.22	0.76	1	0	1	0
11	M12	111	11.24	78.12	0.72	1	0	0	0
12	M7	152	6.56	92.27	0.68	1	0	1	0
13	M11	90	9.31	78.88	0.68	1	0	0	0
14	M10	123	9.26	76.86	0.67	1	0	0	0
15	M3	0	0	0	0	0	0	0	0
16	M5	0	0	0	0	0	0	0	0
17	M15	0	0	0	0	0	0	0	0
18	M17	21	0	0	0	0	0	0	0

- The use of HE, the addition of the B admixture, the SNP superplasticizer, and the coarse sand helped improve the shape stability and the shear stress. The accelerating effect of the SNP resulted in a high shear stress. The cement fineness decreases the flow due to the increased absorption and helps to accelerate the reaction.
- On the other hand, the low sand-to-binder ratio, recycled sand, PCE-2 superplasticizer and high water-to-binder ratio helped increase the flowability. The flow was inversely proportional to the increase in the sand-to-binder ratio, whereas with an increase in the water-to-binder ratio, the workability increases. Additionally, the efficiency of the new generation of superplasticizers is better than that of the old generation, with the PCE-2 being more efficient in terms of workability.
- Mix 4 with HE, fine sand, 0.345 water-to-binder ratio, 2.0 sand-to-binder ratio, PCE-2 superplasticizer and the addition of CSH-C gave the best result, and it was the only mix that met the criteria set. Flowability, shape stability/buildability, and the mechanical properties of the mix were the three criteria. The thresholds were a flow above 60% in 5 min, shear stress above 16 kPa in 90 min, and a compressive strength above 80 MPa in 28 days after the end of the mixing process.

Those 18 mixes were only the initial set of mixes that were formed for these selected materials. This study will continue following optimization and artificial intelligence techniques. The goal is to improve the properties of the mixes following a trend toward multiobjective optimization and narrow down the factors and their levels after identifying the important ones.

Declaration of Competing Interest

The authors declare that they have no known competing financial interests or personal relationships that could have appeared to influence the work reported in this paper.

Acknowledgments

Mr. Pierre Lacroix and Bruce Labrie are thanked for their discussion on the experimental plan. Mr. Sid Ali Sadat is acknowledged for preparing the recycled sand of the project as part of his Master project at ETS. We extend sincere gratitude to Mr. Rios Juan Mauricio, Mr. Victor Brial and Mr. Michael DiMare for providing important recommendations regarding the mix design and the testing methods used in the study. The FRQNT New university researcher grant and the Canada Research Chairs Program supported this study. The Canada Foundation for Innovation - John R. Evans Leaders Fund is also acknowledged.

References

[1] T. Ding, J. Xiao, S. Zou, Y.u. Wang, Hardened properties of layered 3D printed concrete with recycled sand, Cem. Concr. Compos. 113 (2020) 103724.
[2] G. De Schutter, K. Lesage, V. Mechtcherine, V.N. Nerella, G. Habert, I. Agusti-Juan, Vision of 3D printing with concrete — technical, economic and environmental potentials, Cem. Concr. Res. 112 (2018) 25–36.
[3] C. Zhang, V.N. Nerella, A. Krishna, S. Wang, Y. Zhang, V. Mechtcherine, N. Banthia, Mix design concepts for 3D printable concrete: A review, Cem. Concr. Compos. 122 (2021) 104155.
[4] A.V. Rahul, M. Santhanam, Evaluating the printability of concretes containing lightweight coarse aggregates, Cem. Concr. Compos. 109 (2020) 103570.
[5] R. Jayathilakage, P. Rajeev, J.G. Sanjayan, Yield stress criteria to assess the buildability of 3D concrete printing, Constr. Build. Mater. 240 (2020) 117989.
[6] L.i. Wang, Z. Tian, G. Ma, M.o. Zhang, Interlayer bonding improvement of 3D printed concrete with polymer modified mortar: experiments and molecular dynamics studies, Cem. Concr. Compos. 110 (2020) 103571.
[7] G. Ma, Y. Li, L.i. Wang, J. Zhang, Z. Li, Real-time quantification of fresh and hardened mechanical property for 3D printing material by intellectualization with piezoelectric transducers, Constr. Build. Mater. 241 (2020) 117982.
[8] T. Marchment, J. Sanjayan, Mesh reinforcing method for 3D concrete printing, Autom. Constr. 109 (2020) 102992.
[9] D. Marchon, S. Kawashima, H. Bessaies-Bey, S. Mantellato, S. Ng, Hydration and rheology control of concrete for digital fabrication: potential admixtures and cement chemistry, Cem. Concr. Res. 112 (2018) 96–110.
[10] N. Roussel, Rheological requirements for printable concretes, Cem. Concr. Res. 112 (2018) 76–85.
[11] G. Ma, L. Wang, Y. Ju, State-of-the-art of 3D printing technology of cementitious material—an emerging technique for construction, Sci. China Technol. Sci. 61 (4) (2017) 475–495.
[12] C. Ouellet-Plamondon, G. Habert, Life cycle assessment (LCA) of alkali-activated cements and concretes, Handbook of Alkali-Activated Cements, Mortars and Concretes, 2015, pp. 663–686.
[13] R.A. Buswell, W.R. Leal de Silva, S.Z. Jones, J. Dirrenberger, 3D printing using concrete extrusion: a roadmap for research, Cem. Concr. Res. 112 (2018) 37–49.
[14] F. Bos, R. Wolfs, Z. Ahmed, T. Salet, Additive manufacturing of concrete in construction: potentials and challenges of 3D concrete printing, Virt. Phys. Prototyp. 11 (3) (2016) 209–225.
[15] G.H.A. Ting, Y.W.D. Tay, M.J. Tan, Experimental measurement on the effects of recycled glass cullets as aggregates for construction 3D printing, J. Clean. Prod. 300 (2021) 126919.
[16] G.H.A. Ting, Y.W.D. Tay, Y. Qian, M.J. Tan, Utilization of recycled glass for 3D concrete printing: rheological and mechanical properties, J. Mater. Cycles Waste Manage. 21 (4) (2019) 994–1003.
[17] Y.W.D. Tay, Y.e. Qian, M.J. Tan, Printability region for 3D concrete printing using slump and slump flow test, Compos. B Eng. 174 (2019) 106968.
[18] M. Charrier, C.M. Ouellet-Plamondon, Artificial neural network for the prediction of the fresh properties of cementitious materials, Cem. Concr. Res. 156 (2022) 106761.
[19] G. Ma, Z. Li, L. Wang, Printable properties of cementitious material containing copper tailings for extrusion based 3D printing, Constr. Build. Mater. 162 (2018) 613–627.
[20] Y. Zhang, Y. Zhang, G. Liu, Y. Yang, M. Wu, B. Pang, Fresh properties of a novel 3D printing concrete ink, Constr. Build. Mater. 174 (2018) 263–271.
[21] A.V. Rahul, M. Santhanam, H. Meena, Z. Ghani, 3D printable concrete: Mixture design and test methods, Cem. Concr. Compos. 97 (2019) 13–23.
[22] M. Cavazzuti, Optimization methods: from theory to design, Sci. Technol. Aspects Mech. (2013).
[23] J. Lawson, Design and Analysis of Experiments with R, CRC Press Taylor & Francis Group, 2015.
[24] Y. Weng, B. Lu, M. Li, Z. Liu, M.J. Tan, S. Qian, Empirical models to predict rheological properties of fiber reinforced cementitious composites for 3D printing, Constr. Build. Mater. 189 (2018) 676–685.
[25] Z. Liu, M. Li, Y. Weng, T.N. Wong, M.J. Tan, Mixture Design Approach to optimize the rheological properties of the material used in 3D cementitious material printing, Constr. Build. Mater. 198 (2019) 245–255.
[26] I. Ivanova, V. Mechtcherine, Effects of volume fraction and surface area of aggregates on the static yield stress and structural build-up of fresh concrete, Materials (Basel) 13 (7) (2020) 1551.
[27] K.D. Kabagire, A. Yahia, M. Chekired, Toward the prediction of rheological properties of self-consolidating concrete as diphasic material, Constr. Build. Mater. 195 (2019) 600–612.
[28] P. Shakor, J. Renneberg, S. Nejadi, G. Paul, Optimisation of different concrete mix designs for 3D printing by utilizing 6DOF industrial robot, Proceedings of the 34th International Symposium on Automation and Robotics in Construction (ISARC), 2017.
[29] Z. Ge, K. Wang, P.J. Sandberg, J.M. Ruiz, Characterization and performance prediction of cement-based materials using a simple isothermal calorimeter, J. Adv. Concr. Technol. 7 (3) (2009) 355–366.
[30] J. Hu, Z. Ge, K. Wang, Influence of cement fineness and water-to-cement ratio on mortar early-age heat of hydration and set times, Constr. Build. Mater. 50 (2014) 657–663.
[31] D.P. Bentz, Blending different fineness cements to engineer the properties of cement-based materials, Mag. Concr. Res. 62 (5) (2010) 327–338.
[32] K. Ghafor, W. Mahmood, W. Qadir, A. Mohammed, Effect of particle size distribution of sand on mechanical properties of cement mortar modified with microsilica, ACI Mater. J. 117 (1) (2020).
[33] A. Mohammed, N.T.K. Al-Saadi, Ultra-high early strength cementitious grout suitable for additive manufacturing applications fabricated by using graphene oxide and viscosity modifying agents, Polymers (Basel) 12 (12) (2020) 2900.
[34] T.T. Le, S.A. Austin, S. Lim, R.A. Buswell, R. Law, A.G.F. Gibb, T. Thorpe, Hardened properties of high-performance printing concrete, Cem. Concr. Res. 42 (3) (2012) 558–566.
[35] R.J.M. Wolfs, F.P. Bos, T.A.M. Salet, Triaxial compression testing on early age concrete for numerical analysis of 3D concrete printing, Cem. Concr. Compos. 104 (2019) 103344.
[36] R.J.M. Wolfs, F.P. Bos, T.A.M. Salet, Early age mechanical behaviour of 3D printed concrete: numerical modelling and experimental testing, Cem. Concr. Res. 106 (2018) 103–116.
[37] R. Jayathilakage, J. Sanjayan, P. Rajeev, Direct shear test for the assessment of rheological parameters of concrete for 3D printing applications, Mater. Struct. 52 (1) (2019).
[38] J.J. Assaad, J. Harb, Y. Maalouf, Measurement of yield stress of cement pastes using the direct shear test, J. Nonnewton. Fluid Mech. 214 (2014) 18–27.
[39] B.J. Peter Goos, Optimal Design of Experiments – A Case Study Approach.pdf>, Wiley, 2011.

[40] A.C. Atkinson, A.N. Donev, Optimum Experimental Designs, 1992.
[41] V. Sergis, C.M. Ouellet-Plamondon, Fractional factorial design to study admixtures used for 3D concrete printing applications, Materials Letters Submitted, 2021.
[42] Standard Practice for Measuring Hydration Kinetics of Hydraulic Cementitious Mixtures Using Isothermal Calorimetry, C1679 – 17, ASTM International, 2020.
[43] Standard Test Method for Direct Shear Test of Soils Under Consolidated Drained Conditions, D3080 – 04, ASTM International, 2010.
[44] Standard Test Method for Compressive Strength of Hydraulic Cement Mortars (Using 2-in. or [50-mm] Cube Specimens), C109/C109M – 20a, ASTM International, 2020.
[45] .M. Neville, J.J. Brooks, Concrete technology, Longman Scientific & Technical England, 1987.
[46] Standard Test Method for Flow of Hydraulic Cement Mortar, C1437 – 20, ASTM International, 2021.
[47] Standard Specification for Chemical Admixtures for Concrete, C494/C494M – 17, ASTM International, 2018.
[48] J.L. Roy E. Olson, Direct Shear Testing, 2004.
[49] A. ElNemr, Generating water/binder ratio -to- strength curves for cement mortar used in Masnory walls, Constr. Build. Mater. 233 (2020) 117249.
[50] M. Benaicha, X. Roguiez, O. Jalbaud, Y. Burtschell, A.H. Alaoui, Influence of silica fume and viscosity modifying agent on the mechanical and rheological behavior of self compacting concrete, Constr. Build. Mater. 84 (2015) 103–110.
[51] O. Burgos-Montes, M. Palacios, P. Rivilla, F. Puertas, Compatibility between superplasticizer admixtures and cements with mineral additions, Constr. Build. Mater. 31 (2012) 300–309.
[52] G.A. Rao, Role of water-binder ratio on the strength development in mortars incorporated with silica fume, Cem. Concr. Res. 31 (3) (2001) 443–447.
[53] A. ElNemr, Generating water/binder ratio -to- strength curves for cement mortar used in Masnory walls, Constr. Build. Mater. 233 (2020) 117249.
[54] P.C. Aïtcin, 1 - the importance of the water–cement and water–binder ratios, in: P.-C. Aïtcin, R.J. Flatt (Eds.), Science and Technology of Concrete Admixtures, Woodhead Publishing, 2016, pp. 3–13.
[55] P.G.D. Omotola Alawode, O.I. Idowu, Effects of water-cement ratios on the compressive strength and workability of concrete and lateritic concrete mixes, Pacific J. Sci. Technol. 12 (2011).
[56] O. Boukendakdji, E.-H. Kadri, S. Kenai, Effects of granulated blast furnace slag and superplasticizer type on the fresh properties and compressive strength of self-compacting concrete, Cem. Concr. Compos. 34 (4) (2012) 583–590.
[57] J. Kruger, S. Zeranka, G. van Zijl, An ab initio approach for thixotropy characterisation of (nanoparticle-infused) 3D printable concrete, Constr. Build. Mater. 224 (2019) 372–386.
[58] C.A. Anagnostopoulos, T. Chrysanidis, M. Anagnostopoulou, Experimental data of cement grouting in coarse soils with different superplasticisers, Data Brief 30 (2020) 105612.
[59] W. Mahmood, A. Mohammed, K. Ghafor, W. Sarwar, Model technics to predict the impact of the Particle Size Distribution (PSD) of the sand on the mechanical properties of the cement mortar modified with fly ash, Iran. J. Sci. Technol. Trans. Civil Eng. 45 (3) (2020) 1657–1684.
[60] P. Estephane, E.J. Garboczi, J.W. Bullard, O.H. Wallevik, Three-dimensional shape characterization of fine sands and the influence of particle shape on the packing and workability of mortars, Cem. Concr. Compos. 97 (2019) 125–142.
[61] B. Ye, Y. Zhang, J. Han, P. Pan, Effect of water to binder ratio and sand to binder ratio on shrinkage and mechanical properties of high-strength engineered cementitious composite, Constr. Build. Mater. 226 (2019) 899–909.
[62] V. Kanchanason, J. Plank, Effect of calcium silicate hydrate – polycarboxylate ether (C-S-H–PCE) nanocomposite as accelerating admixture on early strength enhancement of slag and calcined clay blended cements, Cem. Concr. Res. 119 (2019) 44–50.